**Zeitschrift:** Helvetica Physica Acta

**Band:** 47 (1974)

**Heft:** 2

**Artikel:** Investigation of the pole graph dominance in the reaction 6Li(p,pd)^4He between 40 and 50 MeV

**Autor:** Beveridge, J.L. / Corfu, R. / Egger, J.P.

**DOI:** https://doi.org/10.5169/seals-114568

Helvetica Physica Acta
Vol. 47, 1974. Birkhäuser Verlag Basel

# Investigation of the Pole Graph Dominance in the Reaction $^6$Li($p,pd$)$^4$He Between 40 and 50 MeV

by **J. L. Beveridge**[1]), **R. Corfu, J. P. Egger, F. Foroughi, J. Piffaretti, J. Rossel** and **E. Schwarz**

Institut de Physique, Université de Neuchâtel, Switzerland

**J. Arvieux, J. L. Durand** and **C. Perrin**

Institut des Sciences Nucléaires, Grenoble, France

(24. I. 74)

*Abstract.* Quasi-free proton–deuteron scattering in the $^6$Li($p,pd$)$^4$He reaction has been investigated in a kinematically complete experiment. The pole graph has been tested by measuring the incident energy dependence of the matrix element between 40 and 50 MeV keeping the invariants of the reaction constant and by applying the Treiman–Yang test at 50 MeV.

## 1. Introduction

The three-body problem, in recent years, has inspired the interest of a large number of physicists, both theoretical and experimental. Unfortunately, the solution of the Faddeev equations, which in principle provide an exact solution to the three-nucleon problem has been in slow progress and even now more or less phenomenological models

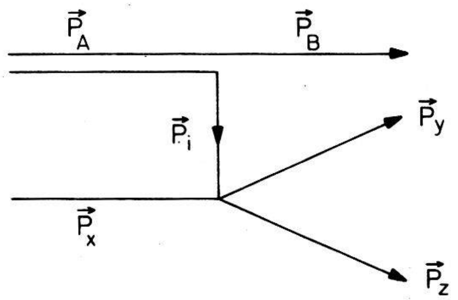


**Figure 1**
Pole graph for the reaction $A(x,yz)B$.

must be used for the interpretation of experimental results. One such model, the impulse approximation (IA) [1], has been used to describe reactions in which one nucleon or cluster of nucleons in the target can be considered to interact freely with the incident particles while the rest of the nucleons remains as a non-interacting spectator. Such a process is known as quasifree scattering (QFS) and can be depicted in the graph formalism as a pole graph of the form of Figure 1.

---

[1]) Present address: University of British Columbia, Vancouver.

In many cases this graph predicts an enhancement at low momentum transfer $\vec{p}_i$ and such enhancements have been observed experimentally. In fact it is found that the shape of the measured cross-sections is reasonably well reproduced by this simple picture of the reaction mechanism even at low incident energies of a few MeV [2] where such a model should be expected to break down. The absolute cross-sections are however poorly predicted at low energy.

A test of the validity of the pole graph, first proposed by Treiman and Yang as a test for the one-pion exchange model [3] and carried over into direct nuclear reactions by Shapiro [4], consists in the verification of the invariance of the squared matrix element under a rotation of the momenta of the particles $z$ and $y$ in the antilaboratory system ($\vec{p}_x = 0$) about the direction of the sum of these momenta (Fig. 2) which is the

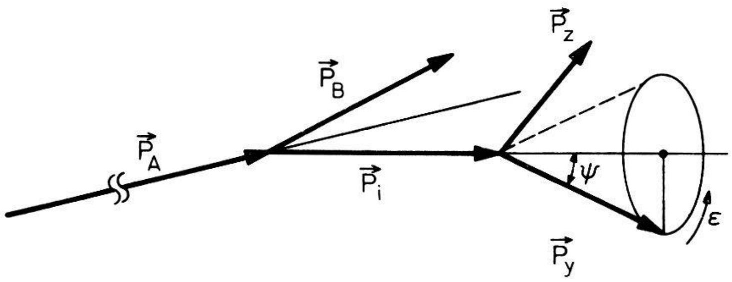


Figure 2
Momentum diagram in the antilaboratory system for the $^6$Li($p$,$pd$)$^4$He reaction corresponding to the pole graph of Figure 1. The momentum of the intermediate deuteron $p_i$ defines the axis of a cone of opening angle $\psi$. $\epsilon$ is the Treiman–Yang angle.

direction of the intermediate particle momentum $\vec{p}_i$. This rotation maintains the invariants found in the pole graph amplitude fixed and thus the predicted matrix element must remain constant for all orientations of the $y$–$z$ plane. The test of the validity of this prediction is referred to as the Treiman–Yang test and the angle of rotation of the $y$–$z$ plane the Treiman–Yang angle (Fig. 2).

This test has the advantage that it does not depend on the exact values of the virtual vertex functions and thus averts problems of 'off-shell' effects. However, the relative momentum for the experimental verification of the criterion must be chosen to be sufficiently large to give a well-defined axis of rotation so that a trivial symmetry around the incident beam is not measured. This condition forces the measurement to be made quite far off the actual QFS peak where the cross-section is low and one has to ensure to be in a kinematical region without other contributions like resonances, final-state interactions, etc. On the other hand, in the case of the $^6$Li($p$,$pd$) $^4$He reaction with a very low $\alpha$-$d$ cluster binding energy ($Q = -1.47$ MeV), the relative momentum must be chosen to be small to satisfy the Shapiro rule of thumb: $q^2 \leqslant 2\mu|Q|$. We have finally adopted a momentum transfer corresponding to an energy of 1.4 MeV for the spectator in the lab system and it seems that this value is a reasonable compromise between the above requirements. In addition, even though a very strong indicator of the dominance of the pole graph in the reaction mechanism, as pointed out by Kolybasov [5] who studied the Treiman–Yang dependence of some triangular graphs, it remains a necessary but not sufficient criterion for this dominance. Since some triangular graphs could also verify the Treiman–Yang criterion Shapiro and Kolybasov [6] proposed an additional test for the pole graph dominance. It is the measurement of the matrix element in function of the incident energy keeping the invariants found in the pole graph amplitude constant. With constant invariants the cross-section divided by the corresponding phase space should not depend on the incident energy. Unfortunately, it is not possible to keep all three invariants constant at all energies. In our case we have left variable the relative energy between the virtually scattered particles in the final state. However, we are very close to the QFS peak with a momentum transfer corresponding to an energy of 0.04 MeV.

## 2. Experimental Set-up

The results presented here were obtained in a series of measurements using proton beams of currents between 50 and 100 nA from the isochronous cyclotron at the Institut des Sciences Nucléaires in Grenoble, incident on 1–2 mg/cm$^2$ 96% pure self-supporting $^6$Li targets placed in a 1.2 m diameter spherical reaction chamber [7]. A schematic diagram of the experimental arrangement is shown in Figure 3. Table 1 gives the geometrical arrangement for the measured points. The detector telescope, 1, which could

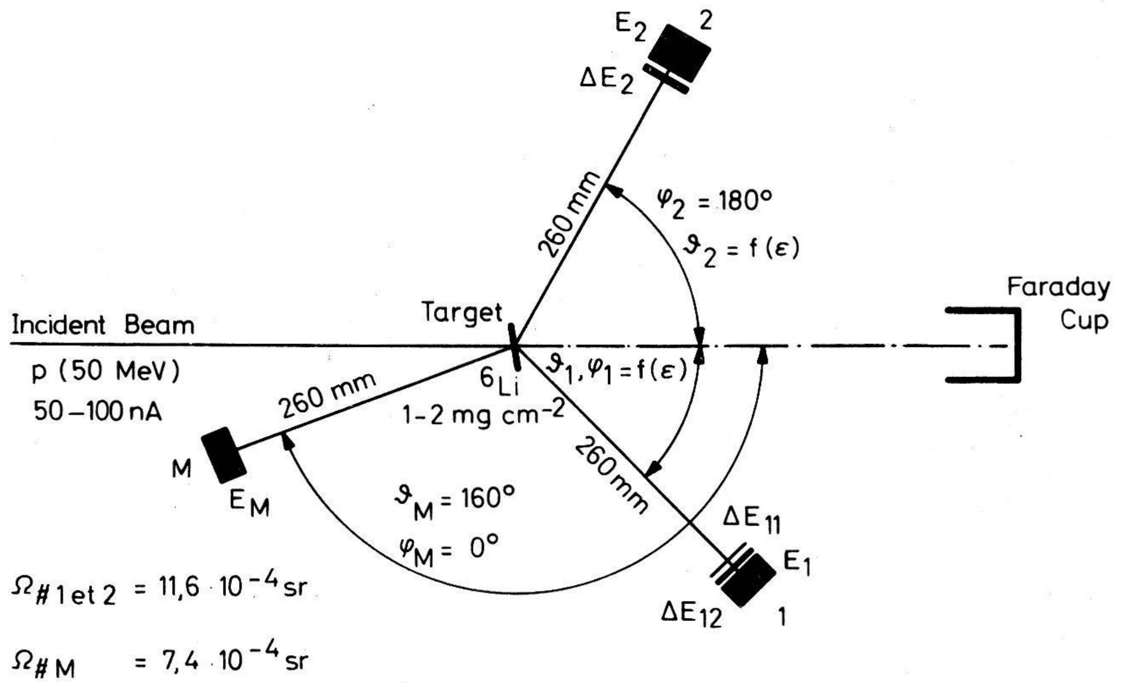


**Figure 3**
Experimental set-up.

Table 1
Experimental energies and angles

| Beam energy (MeV) | $\theta_d$ | Angles $\theta_p$ | Angles $\phi_d - \phi_p$ | Spectator energy (MeV) | Treiman–Yang angle |
|---|---|---|---|---|---|
| 50 | 43° | 88° | 180° | 1.4 | 0° |
| 50 | 42.5° | 85.5° | 160° | 1.4 | 45° |
| 50 | 40° | 80.5° | 152° | 1.4 | 90° |
| 50 | 36° | 76° | 158° | 1.4 | 135° |
| 40 | 38.5° | 66.5° | 166.5° | 0.04 | — |
| 45 | 35.5° | 74.5° | 166° | 0.04 | — |
| 50 | 32.5° | 78.5° | 166.5° | 0.04 | — |

be moved out of the reaction plane, consisted of two silicon surface barrier transmission detectors ($\Delta E$) of 40 and 200 $\mu$m thickness respectively and one 5 mm lithium drifted silicon detector ($E$). This combination allowed the detection and identification of all types of charged particles found in the final state of the $p + {}^6$Li breakup reaction with the following energy limitations

$$5 \text{ MeV} \leqslant E_p \leqslant 30 \text{ MeV}$$
$$6.5 \text{ MeV} \leqslant E_d \leqslant 40 \text{ MeV}$$
$$7.5 \text{ MeV} \leqslant E_t \leqslant 50 \text{ MeV}$$
$$6 \text{ MeV} \leqslant E_{^3\text{He}} \leqslant 50 \text{ MeV}$$
$$7 \text{ MeV} \leqslant E_\alpha \leqslant 50 \text{ MeV}$$

where 50 MeV is the maximum expected energy. The detector telescope, 2, fixed in the reaction plane, consisted of a single $\Delta E$ detector of 200 $\mu$m thickness and one 8 mm (2 × 4 mm in parallel) $E$ detector. This allowed the practical detection and identification only of protons, deuterons and tritons in the energy ranges

$$5 \text{ MeV} \leqslant E_p \leqslant 40 \text{ MeV}$$
$$6.5 \text{ MeV} \leqslant E_d \leqslant 50 \text{ MeV}$$
$$7.5 \text{ MeV} \leqslant E_t \leqslant 50 \text{ MeV}$$

The monitor detector, 4 or 5 mm thickness, was sufficient to stop elastically scattered protons at backward angles of 150 or 160° in the laboratory.

The fast electronics allowed the determination of coincidence events between the two detector telescopes subject to the conditions of coincidence between $\Delta E_{11}$-$\Delta E_{12}$ or $\Delta E_{12}$-$E_1$ in telescope 1 and $\Delta E_2$-$E_2$ in telescope 2. The fast $\Delta E_2$ discriminator pulses, gated by an $E_2$ coincidence, were used as start pulses for a time to amplitude converter (TAC). The gated $\Delta E_{11}$ and $\Delta E_{12}$ pulses OR'ed together and, suitably delayed, provided the stop. A TAC range of 100 nsec allowed the observation of two peaks approximately 20 nsec in width and separated by the cyclotron period. The first contained events due to true and random coincidences between the two telescopes and was used in the data reduction to define a valid coincidence event. The second, due to random events between particles produced by two separate beam pulses, allowed an estimation of the real to random ratio and in the data analysis could be used to determine the background distribution. The event-ratio of the two peaks was about 8 to 1.

The slow electronics and data acquisition system allowed the measurement by six 2000 channel analogue to digital converters (ADC) of the energies $\Delta E_{11}$, $\Delta E_{11} + \Delta E_{12}$, $\Delta E_{11} + \Delta E_{12} + E_1$, $\Delta E_2$, $\Delta E_2 + E_2$ along with the coincidence time spectrum $\Delta t_{12}$. The programmer sequentially transmitted the contents (divided by four) of the ADCs, via an interface, to the PDP 9 for each event which fell within the TAC range (valid stop). Forty events were stored in a buffer by the computer before being transferred onto magnetic tape for off-line analysis. Also, the programmer allowed the transfer of any two preselected ADC contents to the memory of a two-dimensional multichannel analyser (BM 96) enabling the on-line display of the recorded events.

The free spectrum from the detector $E_1$, the monitor spectrum $E_M$ and the coincidence time spectrum $\Delta t_{12}$ were collected on separate multichannel analysers to monitor and control the progress of each experiment.

## 3. Data Reduction and Results

Particle identification in both detector telescopes, which is important due to the number of different particles produced in the final state, was done off-line by means of the two-dimensional spectra $\Delta E$ versus $E$. Events satisfying both particle identification

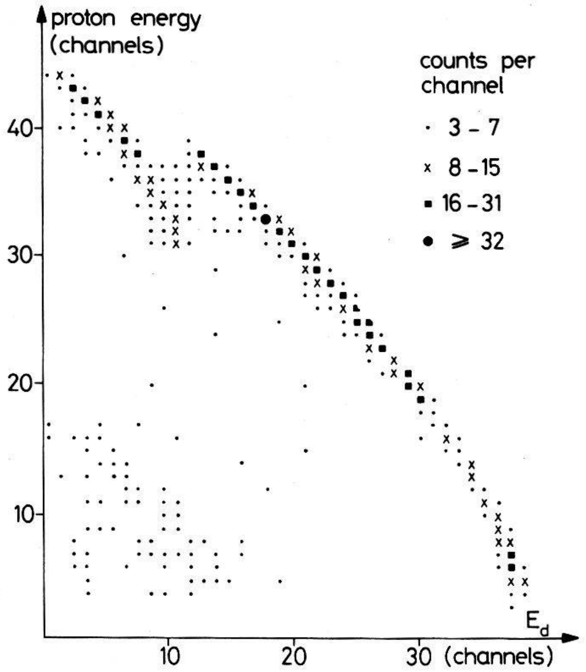


Figure 4

Typical three-body $d$–$p$ kinematic curve corresponding to $E_0 = 50$ MeV and $\epsilon = 90°$ used for the Treiman–Yang test. The lower left corner contains four-body events, probably $p + {}^6Li \to d + p + t + p$ or $p + {}^6Li \to d + p + d + d$ etc. The background is low. The shift in the left of the kinematic curve is due to the use of two 4 mm detectors in parallel in telescope 2, but this is inconsequential because the projection onto the deuteron axis is used for the Treiman–Yang test.

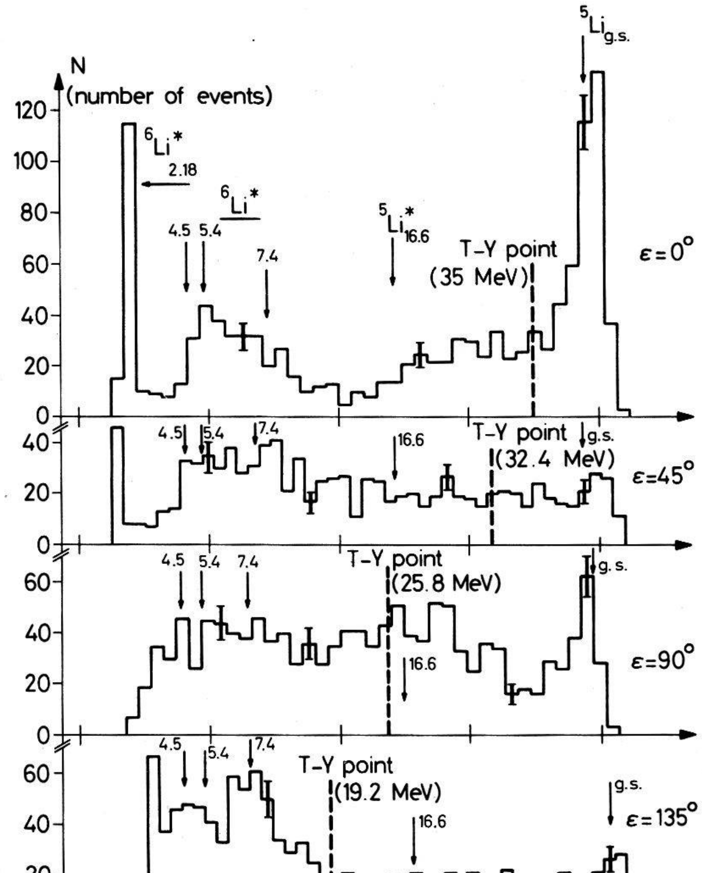


Figure 5

Projection of the three-body $d$–$p$ coincidence events of the four measured Treiman–Yang distributions onto the deuteron energy axis.

and time criteria were arranged in an $E_2$ versus $E_1$ format and printed out as a $64 \times 64$ channel array. In addition to the events on the kinematic curves, some four-body events were detected. In the spectra which were not used for the pole graph test a search for excited $T = \frac{1}{2}$ states in $^3$He by looking for *p–d* final-state interactions has already been made [8]. As an example Figure 4 shows clearly the single three-body *d–p* kinematic curve with some contribution from four-body events and low background. Events along the kinematic curve were then projected on the deuteron energy to give the required

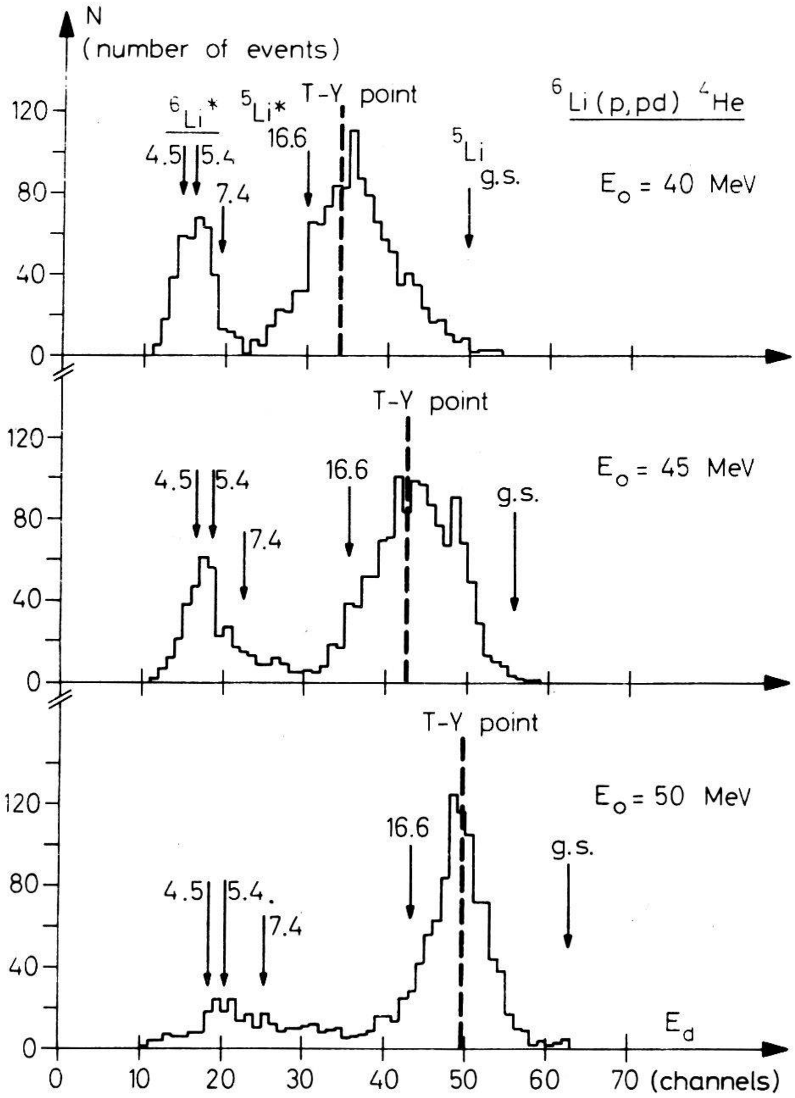


**Figure 6**
**Projection of the three-body *d–p* coincidence events onto the deuteron energy axis for 40, 45 and 50 MeV incident lab energy.**

three-body cross-section $d^3\sigma/dE_1 d\Omega_1 d\Omega_2$. The result is shown in Figure 5. Figure 6 shows the projection for the test with variable incident energy. These spectra exhibit pronounced quasi-free peaks because of the low relative momentum. The location of possible enhancements due to excited states of $^5$Li and $^6$Li are marked, along with the expected position for the Treiman–Yang point. In general, enhancements due to the $^5$Li states are not pronounced and those due to $^6$Li sufficiently removed from the Treiman–Yang point as to not greatly affect measurements in this region.

For the Treiman–Yang test the measurement of interest is the cross-section at the Treiman–Yang point divided by the phase space factor. This quantity, which should be

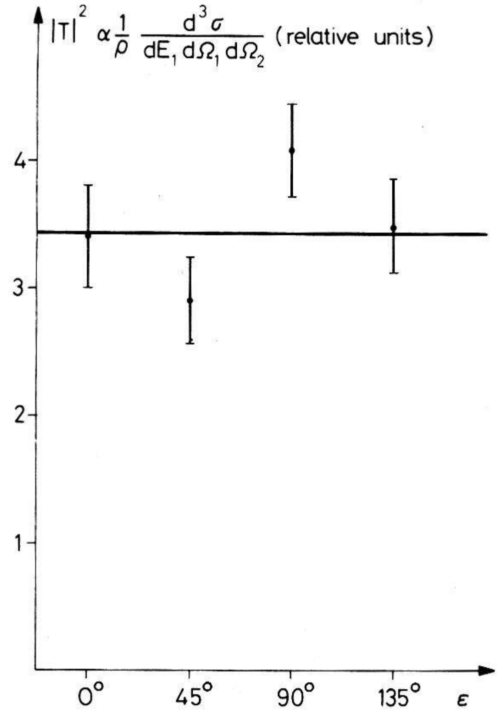


**Figure 7**
Display of the matrix element $|T|^2 \propto (1/\rho)(d^3\sigma/dE_1 d\Omega_1 d\Omega_2)$ as a function of the Treiman–Yang angle $\epsilon$. The horizontal line represents a weighted least square fit of a constant amplitude to the data points. The $\chi^2$ of this fit is 5.2.

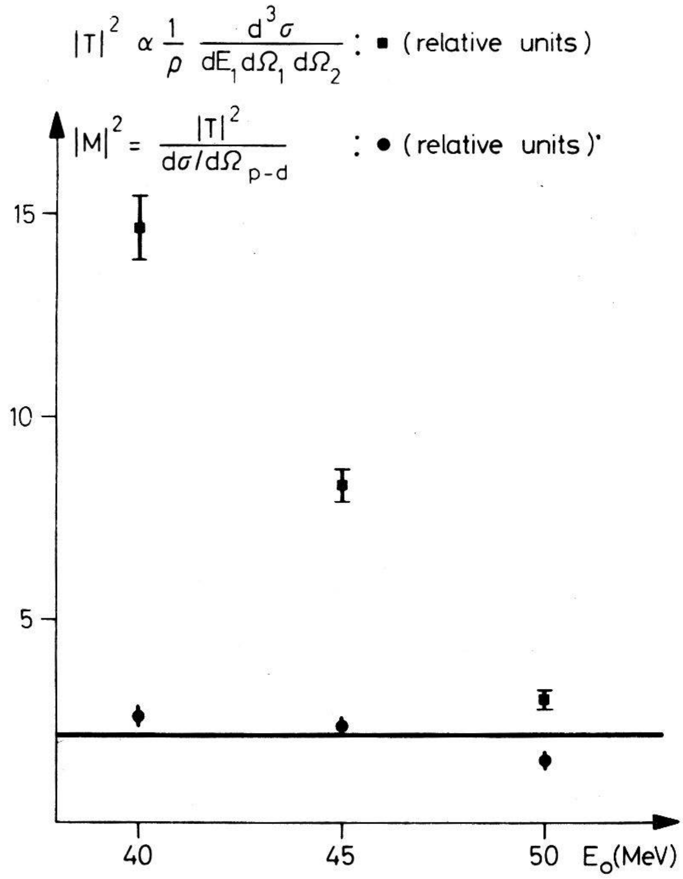


**Figure 8**
Display of the matrix element $|T|^2$ and $|M|^2 = |T|^2/(d\sigma/d\Omega)p - d$ as a function of incident energy according to the numericl values of Table 2. The distribution of $|M|^2 = f(E_0)$ is not flat as indicated by a $\chi^2$ of 5.7.

proportional to the square of the transition matrix element, was extracted by averaging the angular correlation cross-section over four channels (~2.5 MeV) around the Treiman–Yang point and dividing by the phase space factor, which is slowly varying, calculated at that point. Known elastic, inelastic and reaction proton cross-sections on $^6Li$ were used to monitor the different experiments. The results of this procedure are shown in Figure 7 which presents $|T|^2$ in arbitrary units as a function of the Treiman–Yang angle $\epsilon$. The error bars in this figure represent both statistical errors and monitoring errors. The horizontal line of Figure 7 represents a weighted least square fit of a constant amplitude to the data points. The $\chi^2$ of this horizontal line is, within the experimental errors, compatible with the measured points as indicated by the $\chi^2$ of 5.2.

In the experiment in function of incident energy the matrix element was extracted in the same way. Furthermore since the relative $p$–$d$ energy could not be maintained

Table 2
Numerical values for $|T|^2$ and $|M|^2 = |T|^2/[(d\sigma/d\Omega)p - d]$ as a function of incident energy

| Beam energy (MeV) | $\|T\|^2$ (relative units) | $\|M\|^2$ (relative units) |
|---|---|---|
| 40 | 14.62 ± 0.78 | 2.61 ± 0.14 |
| 45 | 8.28 ± 0.42 | 2.37 ± 0.12 |
| 50 | 3.02 ± 0.22 | 1.51 ± 0.11 |

fixed we divided the matrix element by the corresponding free ('on-shell') $p$–$d$ elastic scattering matrix element, which is proportional to the square root of the cross-section. The results of this procedure are presented in Figure 8; we have replaced the squared off-energy-shell matrix element by the corresponding free $p$–$d$ cross-section for the final energy, assuming, as in the impulse approximation, that off-shell effects can be neglected. Table 2 gives the numerical values for $|T|^2$ and $|M|^2 = |T|^2/(d\sigma/d\Omega)\,p$–$d$. The horizontal line of Figure 8 gives a $\chi^2$ of 5.7.

## 4. Discussion

Although the present results do not allow us to draw definitive conclusions, there is some evidence that the pole graph is sufficient to describe the reaction at 50 MeV, as indicated by the invariance of the Treiman–Yang distribution. The slightness of the variation with energy of $|M|^2$ between 40 and 50 MeV shows that the same indication can be extended to this energy range. A previous Treiman–Yang measurement, made at 19 MeV with low momentum transfer [9], gave a similar result.

Let us recall that the Treiman–Yang criterion has been previously applied at lower centre of mass energy to the reactions $H(d, 2p)n$ at 20 MeV [10] and to $^2H(d, pd)n$ also at 20 MeV [11] with negative results.

However, a measurement of the last reaction at 26.5 MeV [12] gave positive results for low momentum transfer.

A measurement of the Treiman–Yang criterion for the $^6Li(p, pd)^4He$ reaction at somewhat lower energy (30–40 MeV), which could be done closer to the QFS peak, would certainly help to clarify the situation. The determination of the relevance of the pole graph in describing this reaction is important as the impulse approximation has been applied in numerous investigations of quasi-free scattering of protons and $\alpha$-particles from $^6Li$ to extract information on the cluster structure of this nucleus [13].

## Acknowledgments

This work was in part supported by the Swiss National Research Foundation and we wish to thank the staff of the Grenoble Cyclotron for their hospitality.

REFERENCES

[1] G. F. CHEW and G. C. WICK, Phys. Rev. *85*, 636 (1951).; G. F. CHEW and M. L. GOLDBERGER, Phys. Rev. *87*, 778 (1952); G. F. CHEW and F. E. LOW, Phys. Rev. *113*, 1640 (1959); A. F. KUCKES, R. WILSON and P. F. COOPER, Annals of Physics *15*, 193 (1961).

[2] A. NIILER, C. JOSEPH, V. VALKOVIC, W. VON WITSCH and G. C. PHILLIPS, Phys. Rev. *182–4*, 1083 (1969).

[3] S. B. TREIMAN and C. N. YANG, Phys. Rev. Lett. *8*, 140 (1962).

[4] I. S. SHAPIRO, V. M. KOLYBASOV and G. R. AUGST, Nucl. Phys. *61*, 353 (1965).

[5] V. M. KOLYBASOV, Sov. Jour. Nucl. Phys. *5*, 202 (1967).

[6] I. S. SHAPIRO and V. M. KOLYBASOV, CERN Trans. *68/13*, 5 (1968).

[7] J. DURISCH, W. NEUMANN and J. ROSSEL, Nucl. Instr. & Meth. *80*, 1 (1970).

[8] J. L. Beveridge, J. P. EGGER, F. FOROUGHI, M. ZAKI, J. L. DURAND, A. FIORE and C. PERRIN, Helv. Phys. Acta *45*, 943 (1972).

[9] R. L. LIEBERT, K. H. PURSER and R. L. BURMAN, *Montreal Conf. on Nucl. Structure* (1969), p. 304, and University of Rochester Report UR-NSRL-55 (June 1972); also in Nucl. Phys. *A136*, 335 (1973).

[10] R. CORFU, J. P. EGGER, C. LUNKE, C. NUSSBAUM, J. ROSSEL, E. SCHWARZ, J. L. DURAND and C. PERRIN, Phys. Rev. Lett. *27*, 1661 (1971).

[11] W. VON WITSCH, W. VIEFERS, H. MOMMSEN, P. DAVID and F. INTERBERGER, Nucl. Phys. *A195*, 617 (1972).

[12] A. D. IJPENBERG, R. VAN DANTZIG, B. J. WIELINJA and I. SLAUS, in *Few Particles Problems* (North Holland, Amsterdam 1972), p. 651.

[13] M. JAIN, P. G. ROOS, H. G. PUGH and H. D. HOLMGREN, Nucl. Phys. *A153*, 49 (1970); H. B. PUGH, J. W. WATSON, D. A. GOLDBERG, P. G. ROOS, D. I. BONBRIGHT and R. A. J. RIDDLE, Phys. Rev. Lett. *22*, 408 (1969); P. G. ROOS, H. KIM, M. JAIN and H. D. HOLMGREN, Phys. Rev. Lett. *22*, 242 (1969); J. R. PIZZI, R. BOUCHÉ, M. GAILLARD, P. GAILLARD, A. GUICHARD, M. GUSAKOV, J. L. LEONHARDT and C. RUHLA, Phys. Lett. *28B*, 32 (1968); D. W. DEVINS et al., Phys. Lett. *9*, 35 (1964); V. VALKOVIC et al., Nucl. Phys. *A106*, 138 (1968); C. RUHLA et al., Phys. Lett. *6* 282 (1963); G. DECONNINK, A. GIORNI, J. P. LONGEQUEUE, J. P. MAILLARD and TSANG UNG CHAN, Phys. Rev. *C3*, 2085 (1971); J. W. WATSON, H. G. PUGH, P. G. ROOS, D. A. GOLDBERG, R. A. J. RIDDLE and D. I. BONBRIGHT, Nucl. Phys. *A172*, 513 (1971); J. M. LAMBERT, R. J. KANE, P. A. TREADO, L. A. BEACH, E. L. PETERSEN and R. B. THEUS, Phys. Rev. *C4*, 2010 (1971); J. C. ALDER, W. DOLLKOPF, W. KOSSLER, C. F. PERDRISAT, W. K. ROBERTS, P. KITCHING, G. A. MOSS, W. C. OLSEN and J. R. PRIEST, Phys. Rev. *C6*, 18 (1972).